

Reduced Order Modeling of Energetic Materials Using Physics-Aware Recurrent Convolutional Neural Networks in a Latent Space (LatentPARC)

Zoë J. Gray^[a], Joseph B. Choi^[a], Youngsoo Choi^[b], H. Keo Springer^[b], H. S. Udaykumar^[c], Stephen S. Baek^{*[a],[d]}

Abstract: Physics-aware deep learning (PADL) has gained popularity for use in complex spatiotemporal dynamics (field evolution) simulations, such as those that arise frequently in computational modeling of energetic materials (EM). Here, we show that the challenge PADL methods face while learning complex field evolution problems can be simplified and accelerated by decoupling it into two tasks: learning complex geometric features in evolving fields and modeling dynamics over these features in a lower dimensional feature space. To accomplish this, we build upon our previous work on physics-aware recurrent convolutions (PARC). PARC embeds knowledge of underlying physics into its neural network architecture for more robust and accurate prediction of evolving physical fields. PARC was shown to effectively learn complex nonlinear features such as the formation of hotspots and coupled shock fronts in various initiation scenarios of EMs, as a function of microstructures, serving effectively as a microstructure-aware burn model. In this work, we further accelerate PARC and reduce its computational cost by projecting the original dynamics onto a lower-dimensional invariant manifold, or ‘latent space.’ The projected latent representation encodes the complex geometry of evolving fields (e.g., temperature and pressure) in a set of data-driven features. The reduced dimension of this latent space allows us to learn the dynamics during the initiation of EM with a lighter and more efficient model. We observe a significant decrease in training and inference time while maintaining results comparable to PARC at inference. This work takes steps towards enabling rapid prediction of EM thermomechanics at larger scales and characterization of EM structure-property-performance linkages at a full application scale.

Keywords: reduced-order modeling, energetic materials, physics-aware deep learning, artificial intelligence

1 Introduction

The study of the relationship between microstructural morphology and sensitivity in energetic materials (EM) is of critical importance as it is directly concerned with the safety of EMs. However, the search space for this problem (i.e., the space of microstructural morphology) is vast, with varying formulations, manufacturing parameters, and such. Experimental methods to study structure-property-performance (SPP) linkages of EMs are often costly and time-consuming,

making numerical simulation an attractive alternative. Direct numerical simulation (DNS) methods, such as SCIMITAR3D [1], [2], [3] use known physics equations (burn models) and rigorous numerical methods to solve those equations. However, DNS remains prohibitively expensive as the complexity of EM thermomechanics demands a finely resolved simulation grid in space and time, limiting our ability to compute only in nano or microscale.

In response to this, our previous work explored the field of physics-aware deep learning (PADL), as a potential enabler for large, application scale modeling of EM thermomechanics. PADL methods leverage the recent success of deep learning with physics knowledge to bridge the gap between the unprecedented cognitive capabilities of modern deep learning algorithms and rigorous scientific requirements in physics research. Beyond the EM community, various PADL models have been shown to successfully model complex spatiotemporal dynamics [4], [5], [6], [7], [8], [9]. Of these, physics-aware recurrent neural networks (PARC) have shown particular promise for challenging nonlinear problems characterized by fast transients, sharp gradients, and discontinuities [5], [6], [10], [11]. Especially regarding EMs, PARC was shown to be capable of rapidly and accurately predicting the formation and growth of hotspots during various initiation scenarios of EMs and characterize EM sensitivity (e.g., James sensitivity envelope) as a function of microstructural morphology [12].

[a] Z.J. Gray, J.B. Choi, S. Baek
School of Data Science
University of Virginia
Charlottesville, VA 22903, United States

[b] Y. Choi, H.K. Springer
Lawrence Livermore National Laboratory
Livermore, CA 94550, United States

[c] H.S. Udaykumar
Department of Mechanical Engineering
University of Iowa
Iowa City, IA 52242, United States

[d] S. Baek
Department of Mechanical and Aerospace Engineering
University of Virginia
Charlottesville, VA 22903, United States

* E-mail: baek@virginia.edu

However, even the state-of-the-art approaches such as PARC, though achieving orders of magnitude speed-ups compared to DNS [5], [6], remain somewhat computationally heavy and slower than ideal yet, to enable large, application scale characterization of EMs. To this end, we focus on the idea of training PARC on the dynamics in a reduced-dimensional latent space, as a promising direction for further optimization. Recent work has shown that projecting high-dimensional data into learned latent spaces before learning dynamics can accelerate surrogate modeling and even improve generalization [13], [14]. These strategies have demonstrated strong performance in relatively simpler physical systems, but their effectiveness is not yet established for problems characterized by sharp gradients, strong nonlinearities, and fast transients such as in EM thermomechanics. Additionally, PARC has not yet been tested on latent-space representations. If such latent-space approaches can preserve the fidelity of PARC in the context of EM, this could be a powerful tool to advance the state of EM modeling and problems in other highly nonlinear physics domains.

In this paper, we introduce LatentPARC, a reduced-order modeling framework that applies PARCv1 in a latent space and achieve both improved predictive performance and significant reductions in inference time and model size. This establishes, for the first time, that PARC models can effectively learn dynamics on a reduced-dimensional data manifold, yielding both speed-up and enhanced flexibility. To situate our contribution, we provide a brief review of relevant literature and build on the prior success of Nguyen et al. [5], [6], which demonstrated the ability to accurately model EM thermo-mechanics such as hot spot formation and growth. Our approach applies deep neural network techniques under the manifold hypothesis, with the goal of retaining PARC’s predictive fidelity while making large-scale exploration of EM design spaces computationally feasible.

2 Background

2.1 Reduced Order Modeling of EMs

In scientific literature, various reduced-order models (ROM) have been proposed. ROMs leverage limited data from a high-fidelity, full-order model (FOM) to construct accurate surrogate models at a fraction of the computational cost. Among ROM strategies for physics modeling, data-driven approaches, which learn directly from data without requiring explicit knowledge of governing equations, are particularly promising since these equations are often unknown or intractable.

However, there is only a limited body of literature on ROM, when it comes to modeling of EM thermomechanics. Most of this limited literature focus on molecular dynamics simulations of EM systems, which, while valuable, address a fundamentally different scale and set of challenges than the mesoscale and macroscale thermomechanics considered here. Most relevant to our present work are of Choi and colleagues [15], [16], who explored modeling EM pore collapse simulations in latent spaces, showing that reduced representations can capture complex pore-collapse dynamics and yield significant computational savings. Our work is complementary, but distinct, in that we embed the physics-aware PARC framework into a latent space using an encoding method compatible with PARC, and work with non-idealized pore geometries.

External to EM literature, most ROM development in physics-informed machine learning has targeted areas such as fluid dynamics [14], [17], [18], [19] and material fracture [14]. These applications, though complex, often involve governing equations and boundary conditions that are more idealized and, in certain respects, simpler than those arising in EM initiation problems.

The motivation LatentPARC is inspired by the manifold hypothesis [20], [21], which suggests that high-dimensional data, despite its complexity, often lies on or near a lower-dimensional manifold embedded within that high-dimensional space. Many methods exist to project data into a reduced-dimensional space and more efficiently capture the essential structure of the

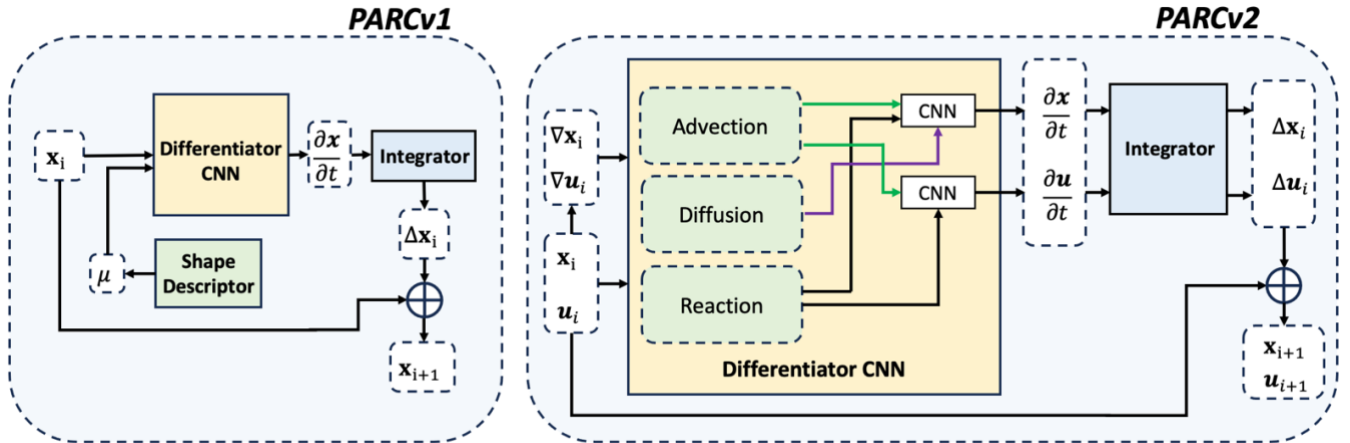


Figure 1: PARCv1 and PARCv2 architectures.

original data. Common approaches include autoencoders [22], proper orthogonal decomposition (POD), dynamic mode decomposition (DMD), diffusion maps [23], and more. For our problem, we employ a convolutional autoencoder due to its computational efficiency, inherent spatial and geometric awareness, and ability to reconstruct the original high-dimensional fields from the latent representation.

2.2 Physics Aware Recurrent Convolutions

Our previous work has demonstrated that PARC can learn the thermomechanics of EMs during various initiation scenarios as a function of microstructure [5], [6], [12], [24]. An imaged microstructure lends itself nicely to computer vision techniques, and as such, PARC works with nonidealized pore geometries, something that was not done with previous methods [16]. PARC, which uses convolutional neural networks (CNN), take geometric and spatial information into account and, as such, is particularly well-suited for modeling field evolution data in physics. PARC leverages CNNs for geometric and spatial feature extraction and function approximation, combined with physics awareness that reduces data requirements, to learn the direct relationship between microstructural morphology and EM initiation phenomena.

The physics awareness of PARC is implemented in the architecture which follows the structure of Equations 1 and 2. The main hypothesis of PARC is that the rate of change $\frac{\partial \mathbf{x}}{\partial t}$ of the state $\mathbf{x} \in X$, where X is the configuration space of evolving physical fields such as temperature and pressure, is a function of the current state \mathbf{x} and the morphology μ , as shown in Equation 1. According to the universal approximation theorem [25], this function f can be accurately approximated by a sufficiently deep neural network, parameterized by the model parameters θ and up to some stochastic noise and prediction error ε . Once f is learned, it can then be used as shown in Equation 2, inspired by classical numerical simulation, to calculate the time integral $\Delta \mathbf{x}$. The computed integral $\Delta \mathbf{x}$ can then be added back to the current state to get the next snapshot of the evolution of \mathbf{x} at the next timestep. Once f is learned, the entire dynamical sequence can be predicted in this manner, by rolling out from an initial condition.

$$\frac{\partial \mathbf{x}}{\partial t} = f(\mathbf{x}, \mu | \theta) + \varepsilon \quad (1)$$

$$\mathbf{x}(t + \Delta t) = \mathbf{x}(t) + \int_0^{\Delta t} f(\mathbf{x}, \mu | \theta) dt \quad (2)$$

The materialization of this idea is illustrated in the architecture of PARCv1 in Figure 1. Here, the key components which we later adapt into the LatentPARC dynamics module are the differentiator CNN, which

learns f and the integrator CNN which learns to integrate f over a time step.

PARCv1 demonstrated the ability to predict the response of shocked microstructures within a 95% confidence band of DNS results, while reducing computation time from hours or days (for DNS) to less than a second [5]. PARCv1 has also been applied to shock-to-detonation transition (SDT) simulations, where it was used to obtain a sensitivity envelope, with high accuracy when verified against an experimentally obtained sensitivity envelop, in just a few hours of work [12].

Building on this foundation, PARCv2 [6] introduces significant advancements over PARCv1. As shown in Figure 1, PARCv2 retains the overall architectural structure of its predecessor but enhances the differentiator with additional physics-based inputs: numerically calculated diffusion and advection fields that constrain the search space towards more physically consistent outputs. PARCv2 has been evaluated across a range of canonical benchmark problems in fluid dynamics, supersonic flow around cylindrical obstacles, shock-induced pore-collapse in EM, and shear band formation in EM under weak shock loading [6], [15]. Across these applications, PARCv2 has consistently outperformed other PADL methods, including PARCv1. The tradeoff, however, is that PARCv2 is substantially heavier, requiring longer to train and having slower inference time than PARCv1.

3 Methods

The LatentPARC architecture assumes that there exists a mapping $f : X \rightarrow Z$ such that the temporal continuity in the original space is preserved in the latent space, i.e., $\frac{\partial \mathbf{x}}{\partial t} \Leftrightarrow \frac{\partial \mathbf{z}}{\partial t}$. Here, $\mathbf{x} \in X$ represents the full order (high-dimensional) physical field data, $\mathbf{z} \in Z$ the reduced order (lower-dimensional) latent representation, and f the encoding function defined by the autoencoder [26]. It is also essential that there exists a mapping $f^{-1} : Z \rightarrow X$ so that, once predictions are made in the reduced Z space, they can be projected back to the full order X space, where measurements and observations can be made. Following this assumption, our goal is to create a model where the latent dynamics retain key temporal features of the physical evolution, enabling efficient learning of spatiotemporal patterns and surrogate modeling of complex systems in a reduced-order form.

3.1 LatentPARC Architecture

The LatentPARC architecture, shown in Figure 2, consists of an encoding module, pictured in green, coupled with a dynamics module adapted from the original PARCv1 architecture, pictured in yellow and blue.

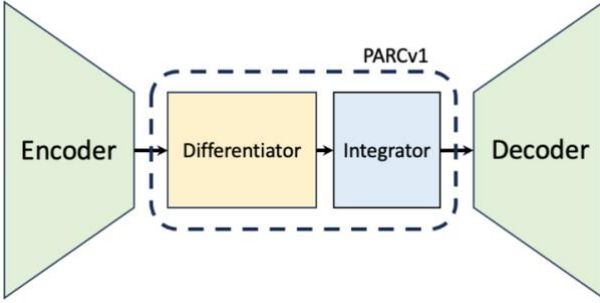


Figure 3: LatentPARC architecture.

In this work, we employ a convolutional autoencoder [26] as the latent encoding module due to its ability to capture key geometric feature information, preserve spatial structure within the latent space, and offer improved efficiency and parameter sparsity compared to fully connected networks. The ability to capture geometric information and preserve an image-like structure in the latent space is essential for the functionality of the PARC module, given that PARC is essentially a computer vision model and operates on image data. Furthermore, the use of a convolutional neural network aligns with our goals of reducing computational cost and memory usage.

The encoder consists of a series of strided convolutional layers [27] and ReLU activations [28], progressively reducing spatial resolution of height and width by 2 times while increasing channel depth. A final bottleneck layer maps the input to the low-dimensional latent space. The decoder mirrors this structure, using bilinear up-sampling followed by convolutional layers to reconstruct the input. This avoids artifacts associated with transpose convolutions while preserving spatial structure. The fully convolutional design ensures parameter efficiency and inductive bias toward local geometric features, making it well suited for modeling physical systems where spatial information is critical.

The dynamics module is modeled after the PARCv1 architecture [5], rather than PARCv2 [6] despite its superior predictive performance. This is because classical advection-diffusion-reaction (ADR) formulations, which are used in the PARCv2 differentiator, are not directly applicable in latent coordinates. In particular, the velocity would need to be implicitly encoded in our current formulation and would therefore not retain a physically interpretable structure after transformation into the latent space. To address this, we adopt the core structure of PARCv1 which does not employ ADR formulations.

Unlike PARCv1, however, our latent-space formulation does not require a separate shape descriptor, since the geometric features of the microstructure are embedded directly into the latent fields alongside temperature and pressure via the convolutional autoencoder. Furthermore, based on prior empirical results, we replace the original CNN-based integrator with a numerical Runge–Kutta integrator (RK4) [29], which has been shown to

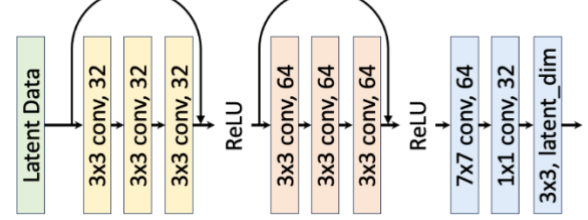


Figure 2: LatentPARC differentiator.

significantly improve PARCv1 prediction accuracy for hotspot formation and nonlinear temporal dynamics. The resulting dynamics module of LatentPARC is thus composed of a residual neural network that estimates the time derivative $\frac{\partial \mathbf{z}}{\partial t}$, followed by RK4 integration to compute $\Delta \mathbf{z}$. The latent state is then updated as described in Equation 3.

$$\mathbf{z}_{k+1} = \mathbf{z}_k + \int_{t_k}^{t_{k+1}} \frac{\partial \mathbf{z}}{\partial t} dt \quad (3)$$

The differentiator CNN, detailed in Figure 3, is composed of two ResNet blocks [30], each containing three 3×3 convolutional layers with skip connections and ReLU activations, designed to capture hierarchical spatial dependencies in the latent representation. This is followed by a 7×7 convolution layer to expand the receptive field and aggregate context, and two 1×1 convolutions for feature channel mixing and dimensionality compression. A final 3×3 convolution layer, inspired by super-resolution, is used to enhance the details [31] of the output of the differentiator, $\frac{\partial \mathbf{z}}{\partial t}$. ReLU activations and dropout are used throughout for regularization and to encourage stable learning of latent dynamics.

3.2 Training the Model

The training of the autoencoder and differentiator components is performed separately. We first train the autoencoder to convergence using the reconstruction loss formula, denoted L_R in Equation 4.1. Here, \mathbf{x}_i denotes the ground truth data and $\bar{\mathbf{x}}_i$ denotes the reconstruction, or output of the decoder. To mitigate over smoothing and encourage the preservation of fine-scale features, we inject additive uniform random noise into the input during training. This approach promotes robustness and helps the model to learn more subtle features that are prevalent in our data. Over the course of training, we use a noise attenuation schedule that gradually decreases the magnitude of the added noise at predefined epoch intervals. This encourages the model to first learn features with larger magnitudes, since lower magnitude features will be obscured by noise, and then learn the finer features as noise is reduced. The addition of this regimen addresses problems specific to the EM dataset which is heterogeneous across channels (microstructure is binary, pressure is relatively normal, and temperature is very skewed). Denoising also helps improve

generalization to unseen samples, an additional advantage given our relatively small training dataset [32].

After training the autoencoder independently, its weights are loaded into the LatentPARC architecture and kept fixed throughout the subsequent training phase. The dynamics module—specifically the differentiator component—is then trained using the dynamics loss function L_D , as defined in Equation 4.2. Here, values with a hat denote a prediction of the dynamics module. Specifically, \hat{z}_{i+1} is the prediction of the next time step within the latent space and \hat{x}_{i+1} is the corresponding decoded version of \hat{z}_{i+1} . The first term in L_D penalizes errors in the predicted latent state at the next time step, encouraging accurate temporal evolution. The second term acts as a regularization constraint, ensuring that the latent trajectories remain within a subspace that can be reliably decoded by the frozen decoder, thereby preserving consistency with the original data manifold.

To train the latent dynamics module, we implemented a rollout training strategy in which the model predicts a sequence of user specified n_{ts} future latent states in an auto-regressive manner. Starting from an initial latent encoding \mathbf{z}_t , the differentiator and numerical integrator are used iteratively to produce $\mathbf{z}_{t+1}, \dots, \mathbf{z}_{t+n_{ts}-1}$. At each time step, the predicted latent state is compared against the corresponding ground truth using the dynamics loss L_D , and the total loss is computed as the average over the full rollout horizon.

This approach allows the model to better capture long-term dependencies, rather than optimizing for one-step prediction accuracy alone. Rollout training is particularly helpful in physical systems where error accumulation over time can lead to unstable or nonphysical behavior. It is also particularly beneficial for physical systems that evolve through distinct phases, each characterized by qualitatively different dynamics, with rapid transitions between them.

$$L_R = \frac{1}{n} \sum_{i=1}^n |\mathbf{x}_i - \bar{\mathbf{x}}_i| \quad (4.1)$$

$$L_D = \frac{1}{n} \sum_{i=1}^n |\mathbf{z}_{i+1} - \hat{\mathbf{z}}_{i+1}| + \frac{1}{n} \sum_{i=1}^n |\mathbf{x}_{i+1} - \hat{\mathbf{x}}_{i+1}| \quad (4.2)$$

3.3 Latent Rollout Prediction

Once LatentPARC is fully trained, predictions can then be made entirely within the latent space. This is what allows for the speedup in inference. To make a prediction with LatentPARC, the initial condition is first encoded, then this latent representation of the initial condition is used by the dynamics module to predict the full sequence of the reaction auto-regressively. Finally, the predicted sequence in the latent space can be decoded by the decoder module to make observations in the original state space.

$$\partial_t \mathbf{z}_t = F(\mathbf{z}_t) \quad (5.1)$$

$$\mathbf{z}_{t+\Delta t} = \int \partial_t \mathbf{z}_t dt \quad (5.2)$$

$$\hat{\mathbf{x}}_t = D(\mathbf{z}_{t+\Delta t}) \quad (5.3)$$

3.4 Quantitative Metrics

To assess the predictive quality of LatentPARC when compared to PARCv1 and PARCv2 in a quantitative manner, we follow the methods detailed in [6]. We evaluate solution quality using the average hotspot temperature and hotspot area, consistent with standard practice in the energetic materials community [33]. These metrics capture both the intensity and spatial extent of hotspot growth, which are critical for assessing initiation behavior. We calculate the RMSE between model prediction and ground truth for six metrics: full temperature field, full pressure field, average temperature of the hotspot (\bar{T}^{hs}), hotspot area (A^{hs}), rate of change of hotspot temperature average ($\dot{\bar{T}}^{hs}$), and rate of change of hotspot area (\dot{A}^{hs}).

3.5 Data

The energetic material (EM) dataset was generated using the SCIMITAR3D code base [1], [2], [3], a direct numerical simulation (DNS) method. The EM dataset consists of 134 instances of a single pore collapse. Each sample consists of 15 time-resolved snapshots of the temperature, pressure, and microstructure fields taken at uniform intervals of $\Delta t = 0.17 \text{ ns}$, capturing the pore collapse and hot spot formation of each sample. The spatial domain spans $1.5 \times 2.25 \mu\text{m}$, with a planar shock of strength $P_s = 9.5 \text{ GPa}$ applied from left to right. The only varying initial condition across samples is the pore geometry, enabling focused study of morphology-driven dynamics under shock loading. Of the 134 total samples, 95 were used for training, 5 for validation, and 34 held out for testing.

4 Results

4.1 Predictive Quality of LatentPARC

To evaluate LatentPARC's predictive ability we compare our model to PARCv1 and PARCv2. We compare LatentPARC to PARCv1, since the latent dynamics module of LatentPARC mimics PARCv1. We compare to PARCv2 because it is the current state-of-the-art model for this EM problem. Each trained model is presented with the initial condition of a sample, unseen during training, which consists of the initial temperature, pressure, and microstructure fields. From this single snapshot, the resultant field evolution snapshots are predicted in an entirely auto regressive manner.

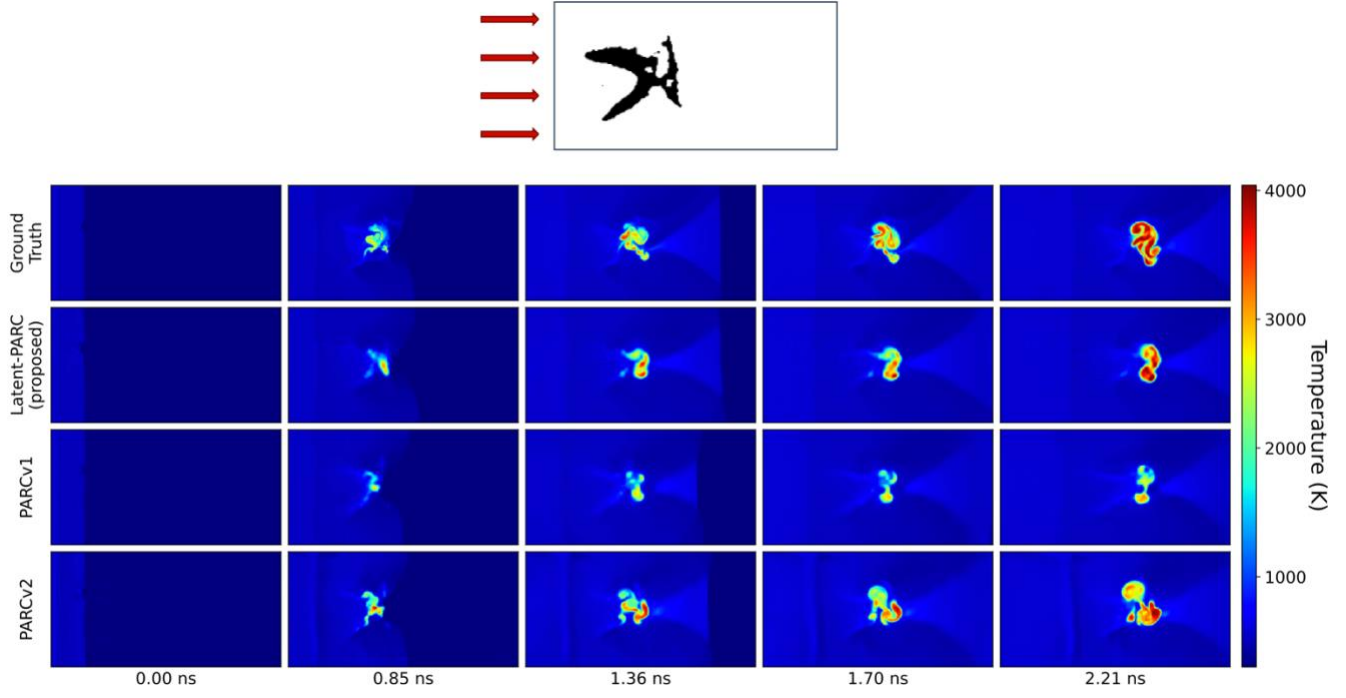


Figure 4: Comparison between temperature field predictions on a test sample.

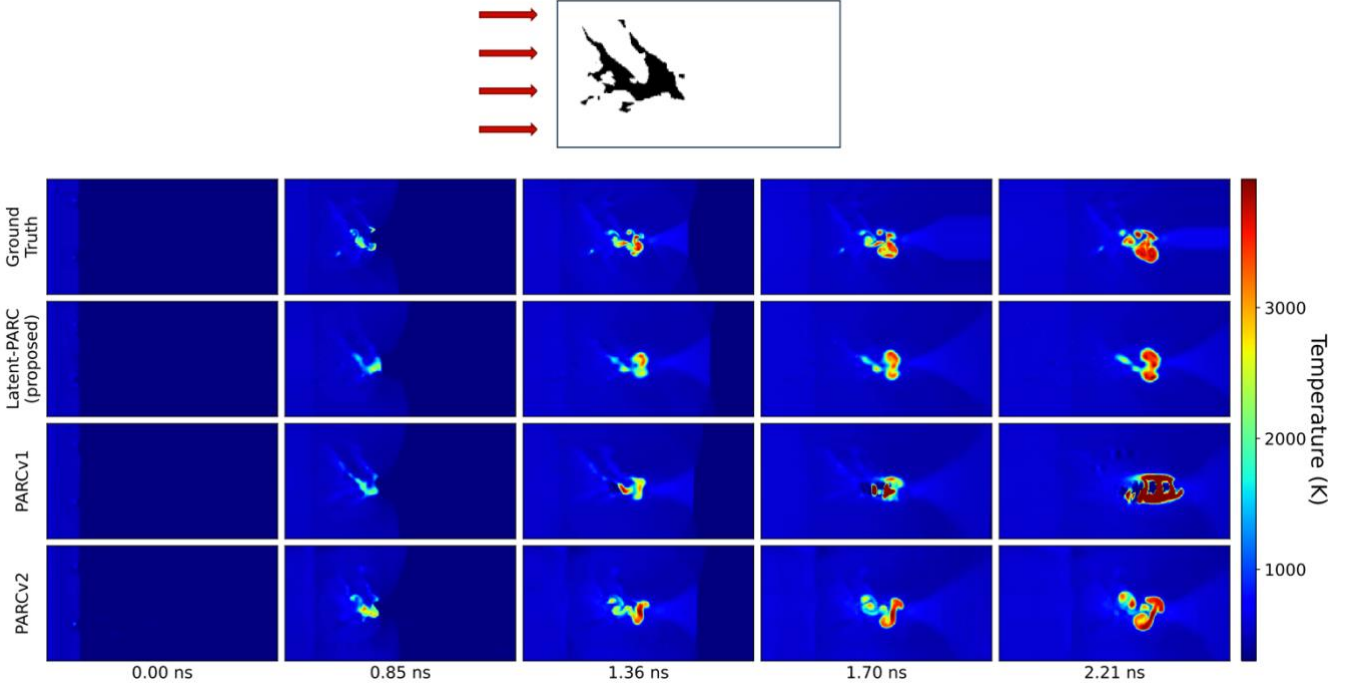


Figure 5: Comparison between temperature field predictions on another test sample.

Figures 4 and 5 demonstrate a qualitative comparison between LatentPARC, PARCv1, PARCv2, and the DNS data which we use as our ground truth. We observe, qualitatively, that LatentPARC captures key features of the reaction such as shock front, hotspot location, hotspot size, and general hotspot geometry with similar ability to PARCv1 and PARCv2. In some cases, LatentPARC captures details of the shock front better than both alternate models. We also observe that LatentPARC is more numerically stable

than PARCv1 during later time steps. For example, PARCv1's prediction in the later time steps in Figure 5 show the beginning stages of error accumulation which result in a corrupted hotspot formation with exceedingly high temperatures. PARCv1 also shows a tendency to underpredict temperature magnitude in later timesteps as observed in Figure 4. LatentPARC does not suffer from either of these issues, and in this sense is closer in quality to PARCv2. However, LatentPARC fails to capture the fine-scale details of

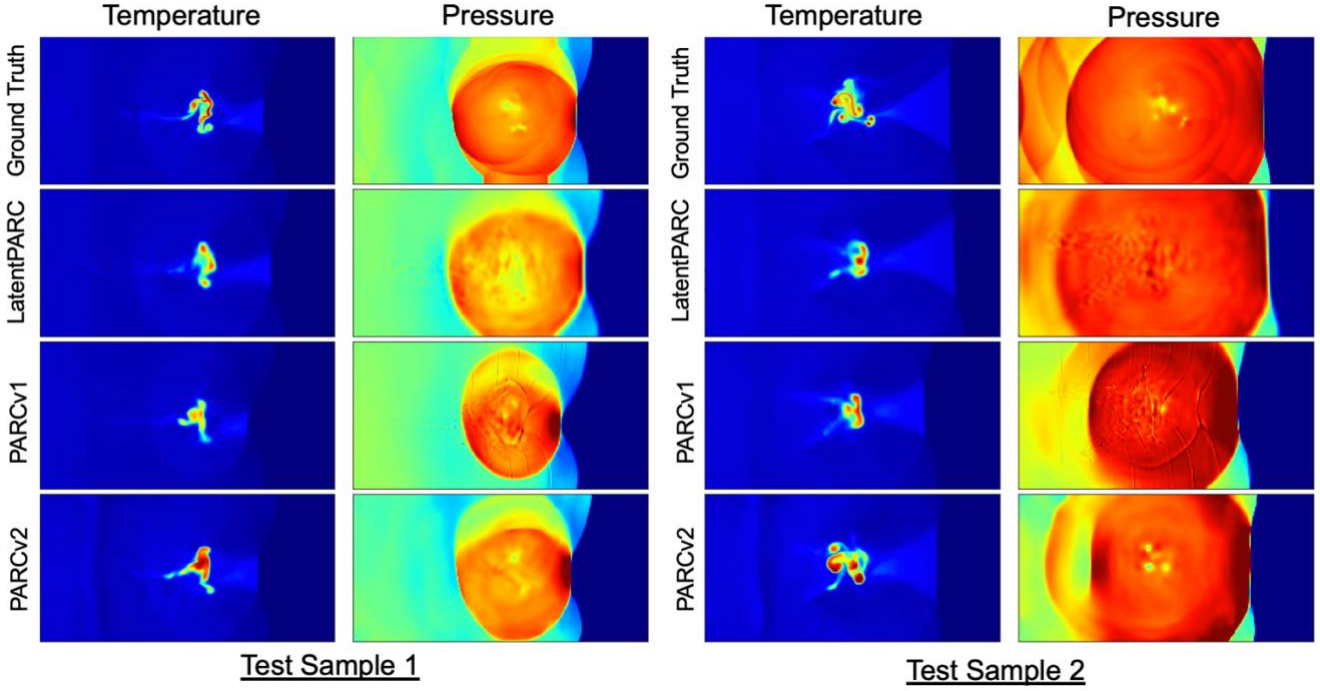


Figure 6: Comparison between temperature and pressure field predictions on two test samples

the hotspot geometry when compared to PARCv2 and tends to produce blurrier predictions than both PARCv1 and PARCv2. This is expected, both since LatentPARC relies on PARCv1 which is also unable to capture these finer details and due to the encoding process being slightly lossy. This discrepancy is acceptable for LatentPARC since it maintains low error in quantitative metrics. However, implementing some version of PARCv2 in the latent space remains a future direction of interest. Since our focus in this study was on establishing the feasibility of reduced-order modeling of the complex spatiotemporal dynamics of EM, we feel this is suitable to leave for future work.

Figure 6 shows a snapshot of the predicted pressure fields in addition to temperature fields on two additional test samples. Here we observe similar trends in model performance on the temperature field predictions. We also, however, note some interesting details in the pressure predictions. We observe that

the pressure field predictions of LatentPARC are blurrier than those of PARCv2 but also don't suffer from artifacts such as those observed in the PARCv1 predictions (vertical bands retained from shock fronts at previous time steps).

Table 1 summarizes the quantitative comparison between LatentPARC, PARCv1, and PARCv2 predictions. As shown, our model achieves an improvement upon PARCv1 in average hotspot temperature, hotspot area, and rate of change of hotspot area. In all other categories, LatentPARC performs similarly to PARCv1. However, the hotspot quantities of interest are of most importance here since they capture the accuracy of physical information that are essential to the usefulness of our model. PARCv2 remains state-of-the-art in all four hotspot metric categories.

	$RMSE T$ (K)	$RMSE P$ (GPa)	$RMSE \bar{T}^{hs}$ (K)	$RMSE A^{hs}$ (μm^2)	$RMSE \dot{\bar{T}}^{hs}$ (K/ns)	$RMSE \dot{A}^{hs}$ ($\mu\text{m}^2/\text{ns}$)
PARCv1	157.18	1.342	378.86	0.0335	678.16	0.0524
PARCv2	186.85	1.438	213.39	0.0324	527.62	0.0420
LATENTPARC	166.42	1.547	307.33	0.0234	688.05	0.0476

Table 1: RMSE of sensitivity quantities of interest for PARCv1, PARCv2 and LatentPARC when compared to ground truth.

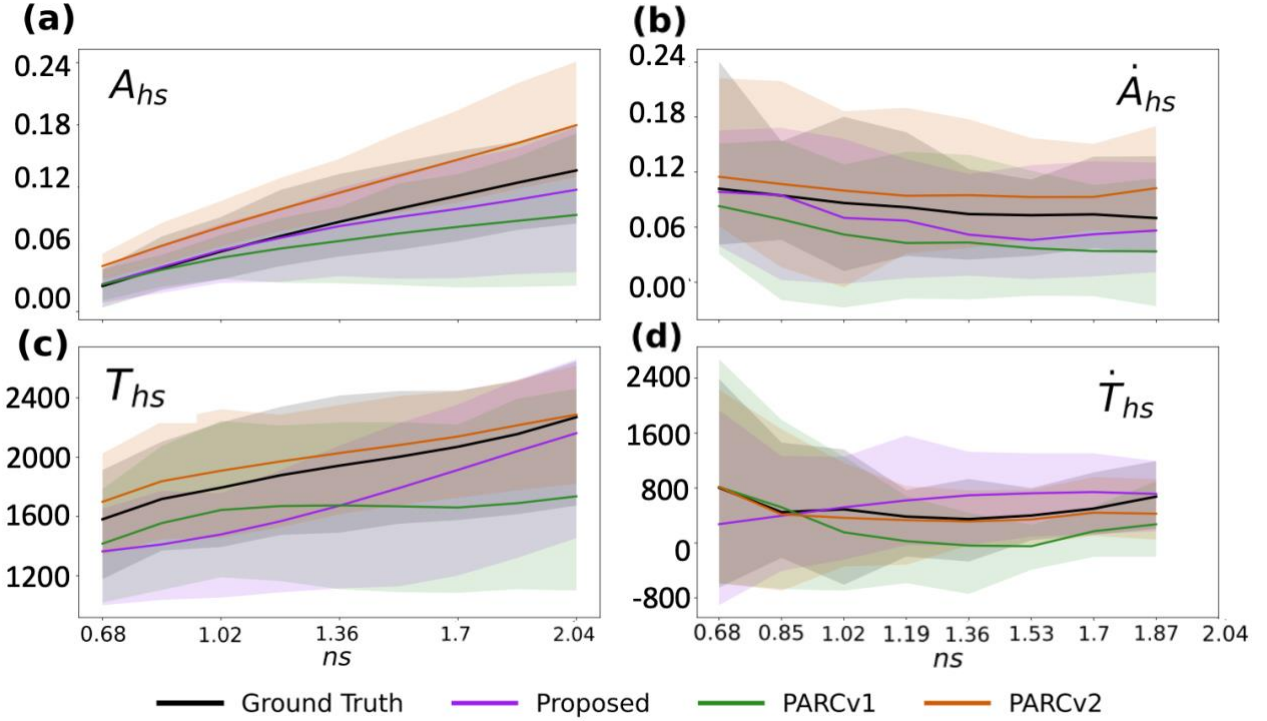


Figure 7: Plots detailing the calculated quantity of interest values across time steps of the prediction.

We detail the trends of our four quantities of interest over the full time series of our model predictions in the plots in Figure 7. Here, we average the performance metrics across all 34 test samples and plot the mean and standard deviation. In these plots, the ground truth is plotted in black, and the closer the value of a model is to that line, the better the model does on that quantity of interest. LatentPARC performs the best of the three models on hotspot area and rate of change of hotspot area. LatentPARC performs better than PARCv1 on average hotspot temperature and about the same on average hotspot temperature rate of change.

4.2 Computational Efficiency of LatentPARC

Once trained, LatentPARC has an inference speed which is roughly 10x and 30x faster than PARCv1 and PARCv2, respectively. In addition to the model speedup, LatentPARC greatly reduces the number of trainable parameters, and thus model size, when compared to previous full order PARC models. Details of these results are specified in Table 2.

	Prediction Speed (GPU)	Trainable Parameters
PARCv1	0.50 s	17,852,019
PARCv2	1.6 s	19,229,509
LATENTPARC	0.045 s	1,264,755

Table 2: Comparison of computational efficiency between PARCv1, PARCv2, and LatentPARC.

5 Discussion

In this work, we introduced LatentPARC, a reduced-order modeling framework for a PARC model that operates in a latent space and apply it to the problem of modeling EM thermomechanics. LatentPARC combines the high predictive fidelity of PARC models with greatly improved computational efficiency and achieves a reduced model size and accelerated inference speed relative to full-order PARC models. LatentPARC's reduced model size positions it as a model with greater flexibility and accessibility than PARCv1 and PARCv2, enabling deployment on resource-constrained hardware such as smaller GPUs without sacrificing the accuracy of PARC models. This opens a possibility to scale PARC to a larger scale simulation of EMs. The significant speed up in inference time when paired with this maintained accuracy makes LatentPARC an ideal tool for making an extensive exploration of the EM design space more feasible.

Given that LatentPARC employs a PARCv1 dynamics module within its latent space, it is notable that our model demonstrates a marked improvement in predictive accuracy over PARCv1. This result supports our hypothesis that projecting our data onto a reduced-dimensional manifold yields dual benefits: (i) the latent representation provides a more compact and structured encoding of the training data, which simplifies the learning of dynamics and improves predictive fidelity; and (ii) the dimensionality reduction itself affords significant gains in computational efficiency and model flexibility. These findings suggest that learning dynamics in a reduced representation space can be advantageous for physics-informed machine learning, even in the absence of explicit constraints on the latent embedding. Importantly, the fact that performance improvements arise despite limited control over the learned latent representation highlights a promising future direction investigating how to learn a latent representation which is explicitly structured to be ideal for the learning of dynamics.

Beyond these immediate computational gains, the results of LatentPARC carry broader implications for the modeling of EMs and for ROM development more generally. The challenge of modeling EMs spans across multitudes of high-dimensional data at multiple scales with strong nonlinear behavior, making it a challenging problem for ROM. By demonstrating that PARC can be successfully projected into a latent space without significant loss in predictive fidelity, we establish that latent neural network-based ROMs are a viable pathway for handling EM thermo-mechanics. Because of this capability, LatentPARC opens the door to rapid simulation at larger scales—both in terms of grid resolution and number of time steps—and provides a foundation for extending PARC-style modeling to full 3D simulations. This advance not only accelerates computational exploration of EM phenomena but also suggests that similar latent-space methods may be extended to other domains with comparable complexity, such as turbulent flows, combustion, and multiphase materials systems.

While LatentPARC demonstrates strong results, several limitations should also be acknowledged. LatentPARC has not yet been tested on problems in other settings. To push LatentPARC further, we would like to test it on EM data with varying initial conditions as well as other physics problems. Applying LatentPARC to single pore EM first was done with the motivation of faster inference time being a priority for EM design exploration and because this is a difficult problem which serves as a convincing comparison to PARC models. Similarly, the current implementation can only explore a limited search space of single-pore geometries. Additionally, once LatentPARC is trained, it can only perform predictions within the initial conditions of its training data. While LatentPARC performs very well on unseen pore geometries, this constraint reduces the practicality of LatentPARC use across initial conditions and material formulations, although it is

important to note that other PARC models and physics informed ML models face similar limitations. Extending LatentPARC to more diverse conditions would require retraining with more extensive data, which remains an area for future work.

6 Conclusion

In this work, we introduced LatentPARC, a reduced-order modeling framework that projects PARC into a latent space to achieve significant efficiency gains while preserving predictive fidelity. By reducing inference time and model size, LatentPARC enables broader and more accessible exploration of energetic material thermo-mechanics, lowering barriers to simulating resultant thermodynamics of complex microstructures thus accelerating EM design. While current limitations, such as fixed initial conditions, single-pore geometries, and reliance on PARCv1 constrain generality, our results demonstrate the feasibility of latent neural network-based ROMs for EM systems and highlight a stable training strategy for balancing reconstruction fidelity with accurate dynamics prediction. Beyond EMs, these findings suggest that latent ROMs offer a scalable pathway for modeling other highly nonlinear, multiscale systems, positioning LatentPARC as both a practical tool for materials scientists and a foundation for future advances in ML-driven reduced-order modeling.

Acknowledgments

This work was performed under the auspices of the U.S. Department of Energy by the Lawrence Livermore National Laboratory under Contract DE-AC52-07NA27344 and was supported by the LLNL-LDRD Program under Project No. 24-SI-004. This work was also partially supported by the National Science Foundation under Grant No. DMREF-2203580. LLNL release number: LLNL-JRNL-2010773.

References

- [1] N. K. Rai, M. J. Schmidt, and H. S. Udaykumar, “High-resolution simulations of cylindrical void collapse in energetic materials: Effect of primary and secondary collapse on initiation thresholds,” *Phys Rev Fluids*, vol. 2, no. 4, p. 043202, Apr. 2017, doi: 10.1103/PhysRevFluids.2.043202.
- [2] N. K. Rai and H. S. Udaykumar, “Mesoscale simulation of reactive pressed energetic materials under shock loading,” *J. Appl. Phys.*, vol. 118, no. 24, p. 245905, Dec. 2015, doi: 10.1063/1.4938581.
- [3] N. K. Rai and H. S. Udaykumar, “Three-dimensional simulations of void collapse in energetic materials,” *Phys Rev Fluids*, vol. 3, no. 3, p. 033201, Mar. 2018, doi: 10.1103/PhysRevFluids.3.033201.

[4] S. L. Brunton, J. L. Proctor, and J. N. Kutz, "Discovering governing equations from data by sparse identification of nonlinear dynamical systems," *Proc. Natl. Acad. Sci.*, vol. 113, no. 15, pp. 3932–3937, Apr. 2016, doi: 10.1073/pnas.1517384113.

[5] P. C. H. Nguyen, Y.-T. Nguyen, J. B. Choi, P. K. Seshadri, H. S. Udaykumar, and S. S. Baek, "PARC: Physics-aware recurrent convolutional neural networks to assimilate meso scale reactive mechanics of energetic materials," *Sci. Adv.*, vol. 9, no. 17, p. eadd6868, doi: 10.1126/sciadv.add6868.

[6] P. C. H. Nguyen *et al.*, "PARCv2: Physics-aware Recurrent Convolutional Neural Networks for Spatiotemporal Dynamics Modeling," in *Proceedings of the 41st International Conference on Machine Learning*, R. Salakhutdinov, Z. Kolter, K. Heller, A. Weller, N. Oliver, J. Scarlett, and F. Berkenkamp, Eds., in *Proceedings of Machine Learning Research*, vol. 235. PMLR, July 2024, pp. 37649–37666. [Online]. Available: <https://proceedings.mlr.press/v235/nguyen24c.html>

[7] P. Ren, C. Rao, Y. Liu, J.-X. Wang, and H. Sun, "PhyCRNet: Physics-informed convolutional-recurrent network for solving spatiotemporal PDEs," *Comput. Methods Appl. Mech. Eng.*, vol. 389, p. 114399, Feb. 2022, doi: 10.1016/j.cma.2021.114399.

[8] G. E. Karniadakis, I. G. Kevrekidis, L. Lu, P. Perdikaris, S. Wang, and L. Yang, "Physics-informed machine learning," *Nat. Rev. Phys.*, vol. 3, no. 6, pp. 422–440, June 2021, doi: 10.1038/s42254-021-00314-5.

[9] M. Raissi, P. Perdikaris, and G. E. Karniadakis, "Physics-informed neural networks: A deep learning framework for solving forward and inverse problems involving nonlinear partial differential equations," *J. Comput. Phys.*, vol. 378, pp. 686–707, Feb. 2019, doi: 10.1016/j.jcp.2018.10.045.

[10] X. Cheng *et al.*, "Physics-aware recurrent convolutional neural networks for modeling multiphase compressible flows," *Int. J. Multiph. Flow*, vol. 177, p. 104877, July 2024, doi: 10.1016/j.ijmultiphaseflow.2024.104877.

[11] M. Kim, N.-K. Chau, S. Park, P. C. H. Nguyen, S. S. Baek, and S. Choi, "Physics-aware machine learning for computational fluid dynamics surrogate model to estimate ventilation performance," *Phys. Fluids*, vol. 37, no. 2, p. 027130, Feb. 2025, doi: 10.1063/5.0251641.

[12] P. C. H. Nguyen, Y.-T. Nguyen, P. K. Seshadri, J. B. Choi, H. S. Udaykumar, and S. Baek, "A Physics-Aware Deep Learning Model for Energy Localization in Multiscale Shock-To-Detonation Simulations of Heterogeneous Energetic Materials," *Propellants Explos. Pyrotech.*, vol. 48, no. 4, p. e202200268, Apr. 2023, doi: 10.1002/prep.202200268.

[13] W. D. Fries, X. He, and Y. Choi, "LaSDI: Parametric Latent Space Dynamics Identification," *Comput. Methods Appl. Mech. Eng.*, vol. 399, p. 115436, Sept. 2022, doi: 10.1016/j.cma.2022.115436.

[14] K. Kontolati, S. Goswami, G. Em Karniadakis, and M. D. Shields, "Learning nonlinear operators in latent spaces for real-time predictions of complex dynamics in physical systems," *Nat. Commun.*, vol. 15, no. 1, p. 5101, June 2024, doi: 10.1038/s41467-024-49411-w.

[15] S. W. Chung, C. Miller, Y. Choi, P. Tranquilli, H. K. Springer, and K. Sullivan, "Latent Space Dynamics Identification for Interface Tracking with Application to Shock-Induced Pore Collapse," July 14, 2025, *arXiv*: arXiv:2507.10647. doi: 10.48550/arXiv.2507.10647.

[16] S. W. Cheung, Y. Choi, H. K. Springer, and T. Kadeethum, "Data-scarce surrogate modeling of shock-induced pore collapse process," *Shock Waves*, vol. 34, no. 3, pp. 237–256, June 2024, doi: 10.1007/s00193-024-01177-2.

[17] S. Karumuri, L. Graham-Brady, and S. Goswami, "Physics-Informed Latent Neural Operator for Real-time Predictions of Complex Physical Systems," June 13, 2025, *arXiv*: arXiv:2501.08428. doi: 10.48550/arXiv.2501.08428.

[18] F. Regazzoni, S. Pagani, M. Salvador, L. Dede', and A. Quarteroni, "Learning the intrinsic dynamics of spatio-temporal processes through Latent Dynamics Networks," *Nat. Commun.*, vol. 15, no. 1, p. 1834, Feb. 2024, doi: 10.1038/s41467-024-45323-x.

[19] T. Wang and C. Wang, "Latent Neural Operator for Solving Forward and Inverse PDE Problems," Dec. 20, 2024, *arXiv*: arXiv:2406.03923. doi: 10.48550/arXiv.2406.03923.

[20] P. P. Brahma, D. Wu, and Y. She, "Why Deep Learning Works: A Manifold Disentanglement Perspective," *IEEE Trans. Neural Netw. Learn. Syst.*, vol. 27, no. 10, pp. 1997–2008, Oct. 2016, doi: 10.1109/TNNLS.2015.2496947.

[21] L. Clayton, "Algorithms for manifold learning," *C San Diego Dep. Comput. Sci. Eng.*, 2008, [Online]. Available: <https://escholarship.org/uc/item/8969r8tc>

[22] D. Bank, N. Koenigstein, and Raja Giryes, "Autoencoders," Apr. 03, 2021, *arXiv*: arXiv:2003.05991. doi: 10.48550/arXiv.2003.05991.

[23] R. R. Coifman and S. Lafon, "Diffusion maps," *Spec. Issue Diffus. Maps Wavelets*, vol. 21, no. 1, pp. 5–30, July 2006, doi: 10.1016/j.acha.2006.04.006.

[24] Stephen S. Baek *et al.*, "Predicting Shock Initiation Threshold Using Physics-Aware Deep Learning Models," presented at the The 17th International Detonation Symposium, Kansas City, Missouri, 2024.

[25] G. Cybenko, "Approximation by Superposition of a Sigmoidal Function," *Mathematics of Control, Signals, and Systems*, 1989.

[26] U. Meier, D. Cireşan, and J. Schmidhuber, "Stacked Convolutional Auto-Encoders for Hierarchical Feature Extraction," in *Artificial Neural Networks and Machine Learning – ICANN 2011*, vol. 6791, T. Honkela, W. Duch, M. Girolami, and S. Kaski, Eds., in Lecture Notes in Computer Science, vol. 6791. , Berlin, Heidelberg: Springer Berlin Heidelberg, 2011, pp. 52–59. doi: 10.1007/978-3-642-21735-7_7.

[27] Y. LeCun *et al.*, "Backpropagation Applied to Handwritten Zip Code Recognition," *Neural Comput.*, vol. 1, no. 4, pp. 541–551, Dec. 1989, doi: 10.1162/neco.1989.1.4.541.

[28] V. Nair and G. E. Hinton, "Rectified linear units improve restricted boltzmann machines," in *Proceedings of the 27th International Conference on International Conference on Machine Learning*, in ICML'10. Madison, WI, USA: Omnipress, 2010, pp. 807–814.

[29] J. C. Butcher, "A history of Runge-Kutta methods," *Appl. Numer. Math.*, vol. 20, no. 3, pp. 247–260, Mar. 1996, doi: 10.1016/0168-9274(95)00108-5.

[30] K. He, X. Zhang, S. Ren, and J. Sun, "Deep Residual Learning for Image Recognition," in *2016 IEEE Conference on Computer Vision and Pattern Recognition (CVPR)*, Las Vegas, NV, USA: IEEE, June 2016, pp. 770–778. doi: 10.1109/CVPR.2016.90.

[31] C. Dong, C. C. Loy, K. He, and X. Tang, "Image Super-Resolution Using Deep Convolutional Networks," *IEEE Trans. Pattern Anal. Mach. Intell.*, vol. 38, no. 2, pp. 295–307, Feb. 2016, doi: 10.1109/TPAMI.2015.2439281.

[32] P. Vincent, H. Larochelle, Y. Bengio, and P.-A. Manzagol, "Extracting and composing robust features with denoising autoencoders," in *Proceedings of the 25th international conference on Machine learning - ICML '08*, Helsinki, Finland: ACM Press, 2008, pp. 1096–1103. doi: 10.1145/1390156.1390294.

[33] Y. Nguyen, P. Seshadri, O. Sen, D. B. Hardin, C. D. Molek, and H. S. Udaykumar, "Multi-scale modeling of shock initiation of a pressed energetic material I: The effect of void shapes on energy localization," *J. Appl. Phys.*, vol. 131, no. 5, p. 055906, Feb. 2022, doi: 10.1063/5.0068715.